AgriChrono: A Multi-modal Dataset Capturing Crop Growth and Lighting Variability with a Field Robot

Jaehwan Jeong[1,2], Tuan-Anh Vu[2], Mohammad Jony[3], Shahab Ahmad[3], Md. Mukhlesur Rahman[3], Sangpil Kim[1,*], and M. Khalid Jawed[2,*]

***Abstract*— Existing datasets for precision agriculture have primarily been collected in static or controlled environments such as indoor labs or greenhouses, often with limited sensor diversity and restricted temporal span. These conditions fail to reflect the dynamic nature of real farmland, including illumination changes, crop growth variation, and natural disturbances. As a result, models trained on such data often lack robustness and generalization when applied to real-world field scenarios. In this paper, we present AgriChrono, a novel robotic data collection platform and multi-modal dataset designed to capture the dynamic conditions of real-world agricultural environments. Our platform integrates multiple sensors and enables remote, time-synchronized acquisition of RGB, Depth, LiDAR, and IMU data, supporting efficient and repeatable long-term data collection across varying illumination and crop growth stages. We benchmark a range of state-of-the-art 3D reconstruction models on the AgriChrono dataset, highlighting the difficulty of reconstruction in real-world field environments and demonstrating its value as a research asset for advancing model generalization under dynamic conditions. The code and dataset are publicly available at: `https://github.com/StructuresComp/agri-chrono`**

I. Introduction

The rapid advancement of AI has accelerated the use of autonomous robotic systems in precision agriculture for tasks such as crop monitoring, condition assessment, and automated field operations [1]. However, the datasets available for training and evaluating these systems remain limited in both diversity and realism. Most existing datasets are object-centric or collected in controlled environments such as indoor labs or greenhouses, where the scene lacks the complexity of real farmland [2], [3]. Furthermore, data collection is often limited to a single short-term session, without capturing temporal progression. As a result, these datasets fail to represent variations in natural illumination and the morphological changes that occur throughout crop growth, limiting model generalization to real-world agricultural environments.

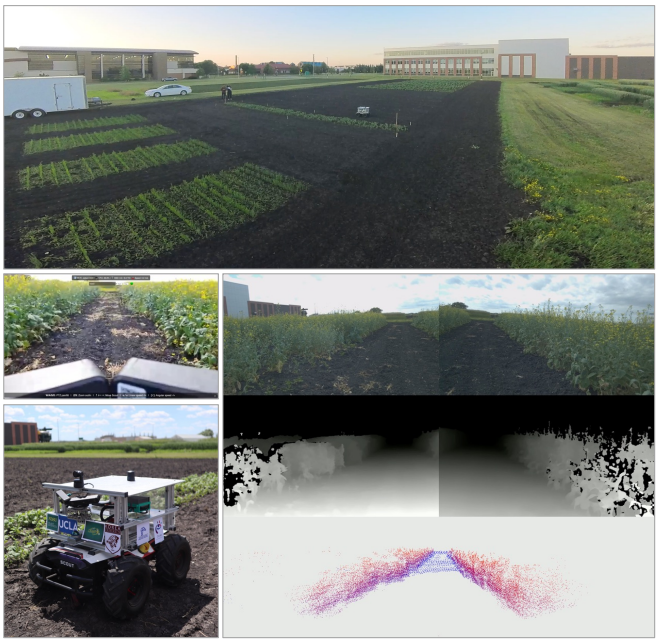

Fig. 1: Overview of the *AgriChrono* field-scale data collection framework. **Top,** a real-world outdoor agricultural field used for data acquisition. **Middle left,** user interface for remote robot control and data collection. **Bottom left,** robotic platform with multiple sensors for field data collection. **Bottom right,** time-aligned multi-modal frame with RGB, Depth, and LiDAR data.

To address these gaps, we introduce *AgriChrono*, a robotic platform and multi-modal dataset designed to reflect the structural, temporal, and environmental complexity of real agricultural scenes (Fig. 1). Our mobile ground robot is equipped with two stereo camera units and a LiDAR sensor, along with supporting modules integrated into a single onboard system. The platform ensures stable and synchronized acquisition of four-view RGB, two-view depth, LiDAR, and IMU data. It also supports long-range remote communication, real-time streaming, and efficient logging, enabling high-quality, long-term data collection while reducing operator workload. Using this platform, we collected a one-month dataset across three crop field sites containing canola, flax, and a genotype variant of canola. The dataset captures diverse lighting conditions and structural variation throughout the crop growth cycle, comprising a total of 175 sessions and

This work was supported in part by the US Department of Agriculture (grant numbers 2024-67021-42528 and 2022-67022-37021), the Culture, Sports, and Tourism R&D Program through the Korea Creative Content Agency grant funded by the Ministry of Culture, Sports and Tourism in 2024 (International Collaborative Research and Global Talent Development for the Development of Copyright Management and Protection Technologies for Generative AI, RS-2024-00345025), and the Institute of Information & Communications Technology Planning & Evaluation (IITP) grant funded by the Korea government (MSIT) (No. RS-2019-II190079, Artificial Intelligence Graduate School Program, Korea University).

[1] Department of Artificial Intelligence, Korea University, Seoul 02841, Republic of Korea. J. Jeong is also a visiting scholar at the University of California, Los Angeles, CA, USA. {jhwan, spk7}@korea.ac.kr

[2] Department of Mechanical & Aerospace Engineering, University of California, Los Angeles, CA 90095, USA. tuananh.vu@ucla.edu, khalidjm@seas.ucla.edu

[3] Department of Plant Sciences, North Dakota State University, Fargo, ND 58102, USA. {mohammad.jony, shahab.ahmad, md.m.rahman} @ndsu.edu

[*] Co-corresponding authors.

Dataset	Modalities	Data Target	Time Aligned	Growth Span	Lighting Variance	Open-field	Size
Agroscapes [4]	RGB	Scene-level	-	✗	✗	✓	9 GB
NIRPlant [5]	RGB, Depth, NIR, LiDAR	Object-level	✗	✗	✓	✗	554 GB
BonnBeetCloud3D [6]	RGB	Scene-level	-	✗	✗	✓	10 GB
Crops3D [7]	RGB, TLS, SL	Scene-level	✗	✗	✗	✓	9 GB
PlantSegNet [8]	Geometry∗	Scene-level	✓	✓	✓	✗	N/A∗
AgriChrono	**RGB, Depth, LiDAR, IMU**	**Scene-level**	✓	✓	✓	✓	**18 TB**

TABLE I: Comparison of related agricultural datasets in terms of sensor configurations and spatio-temporal coverage. Unlike previous datasets, *AgriChrono* offers synchronized RGB, Depth, LiDAR, and IMU data, captured as time-series over multiple growth stages and varying lighting conditions in real open-field environments. This comprehensive setup supports advanced research for spatio-temporal crop analysis, 3D reconstruction, and multi-modal field-level modeling under realistic and diverse farming scenarios.
∗ Synthetic dataset generated via simulation.

totaling approximately 18 TB. Benchmarking state-of-the-art 3D reconstruction models on *AgriChrono* highlights the difficulty of reconstruction in dynamic outdoor environments and demonstrates its value as a research asset for advancing model generalization in real-world scenarios.

The main contributions of this work are as follows:

- We develop a real-world robotic data collection platform tailored for precision agriculture, integrating time-synchronized RGB-D cameras, LiDAR, and IMUs with remote operation and real-time monitoring to enable efficient, long-term deployment.
- We construct *AgriChrono*, a large-scale multi-modal dataset collected over one month across three crop types, comprising a total of 175 sessions under varying illumination and growth conditions.
- We benchmark state-of-the-art 3D reconstruction models on *AgriChrono*, highlighting reconstruction challenges and its utility for improving model robustness and generalization.

II. Related Work

Agroscapes [4] provides video-based RGB imagery collected across large-scale farmlands using UAVs, handheld, and ground-based platforms for crop monitoring. However, it is limited to RGB-only modality and was captured within a narrow temporal window, lacking scene diversity related to illumination changes and crop growth variation.

NIRPlant [5] includes a wide range of sensing modalities such as RGB, Depth, NIR, and LiDAR with multi-view images captured from 36 viewpoints. Although it supports four lighting conditions, the dataset was acquired using an automated turntable system in a controlled indoor setting. It is confined to single-object scenes, which limits both realism and applicability to field-level perception.

BonnBeetClouds3D [6] focuses on phenotyping with crop-specific point cloud data. While it provides detailed static structural information of individual plants, the dataset was collected under fixed crop arrangements and limited temporal conditions. As a result, it lacks sufficient visual diversity and realistic scene complexity arising from illumination changes, morphological growth, and natural crop motion.

Crops3D [7] offers RGB, terrestrial LiDAR (TLS), and structured light scans collected from real farm environments, providing strength in modality diversity. However, it depends on tripod-based static capture, suffers from frame-level temporal misalignment, and lacks temporal continuity across growth stages. Its fixed-position acquisition strategy limits scalability for capturing spatial and temporal dynamics in large agricultural fields. In addition, the collection process demands considerable manual effort, as the equipment must be manually moved to capture different viewing angles.

PlantSegNet [8] is a fully synthetic dataset procedurally generated with 360-degree multi-view scans and fine-grained semantic and instance labels. It does not include RGB or sensor-derived signals, and all scenes are rendered in simulated environments, which limits its realism and transferability to real-world applications.

Overall, existing datasets commonly suffer from static or non-realistic settings, limited temporal or spatial scope, incomplete modality coverage, and the absence of dynamic crop behavior (Table I). These limitations hinder the development of generalizable models and underscore the need for realistic agricultural data and a scalable collection platform capable of enabling such data acquisition.

III. Methods

A. System Architecture

Robotic Platform Design. Our *AgriChrono* platform is a fully integrated field robot designed for long-term data collection in outdoor agricultural environments. The system is built on the AgileX Scout 2.0 unmanned ground vehicle (UGV) and integrates a tiered sensor suite, an onboard compute unit, and a wireless communication module. At the bottom tier, a Livox Mid-360 LiDAR is mounted to leverage its asymmetric vertical field of view (-7° to $+52^\circ$), ensuring reliable ground-level perception. As the upper FoV beyond $+52^\circ$ is inherently occluded, this placement avoids occlusion and enables unobstructed acquisition of forward-facing crop point clouds without interference from upper components. The middle tier consists of two ZED X stereo cameras mounted on vibration-isolating and tilt-adjustable heads. The cameras are positioned with a 130° outward angle between them, yielding a combined 150° horizontal field of view for wide-baseline, multi-view RGB-D capture. The isolation system mitigates high-frequency vibrations induced by onboard electronics, while the tilt mechanism adapts to crop growth stages, enabling robust perception across field conditions. At the top tier, an OBSBOT Tail

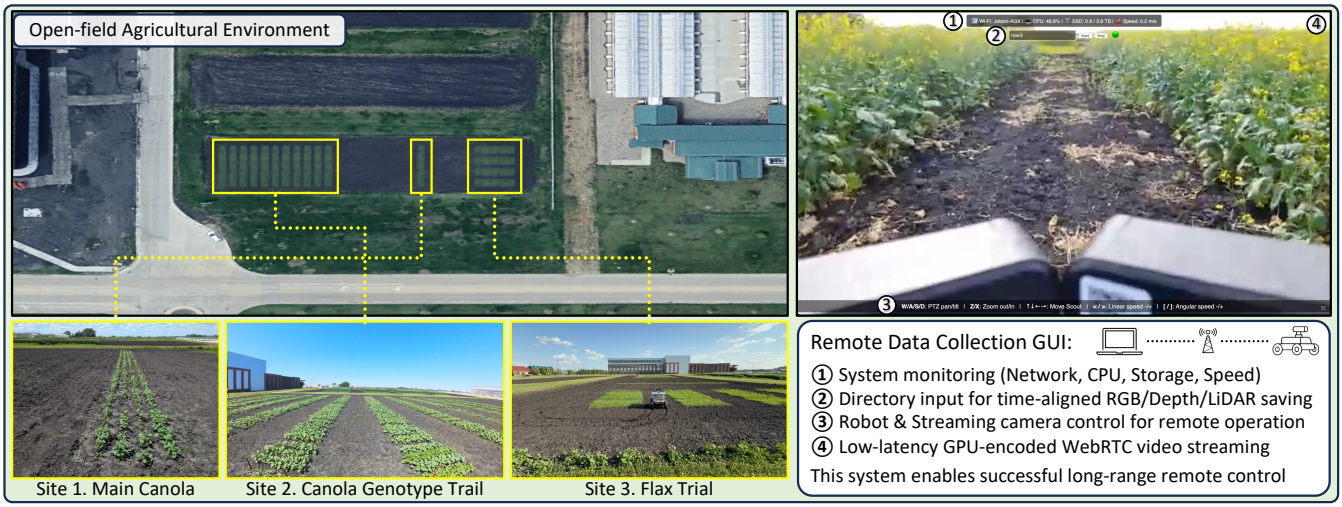

Fig. 2: Data collection sites and the remote operation interface used during field trials. **Site 1,** main canola site used as the primary location for repeated data collection, capturing temporal changes in illumination and crop structure. **Site 2,** genotype trial site featuring diverse canola varieties, enabling the capture of morphological variation across crop types. **Site 3,** flax trial site composed of multiple plots with varying weed control strategies, providing structural diversity in a controlled multi-block layout. **GUI,** remote interface supporting real-time system feedback, intuitive directory-based data saving, responsive robot and camera control, and low-latency teleoperation.

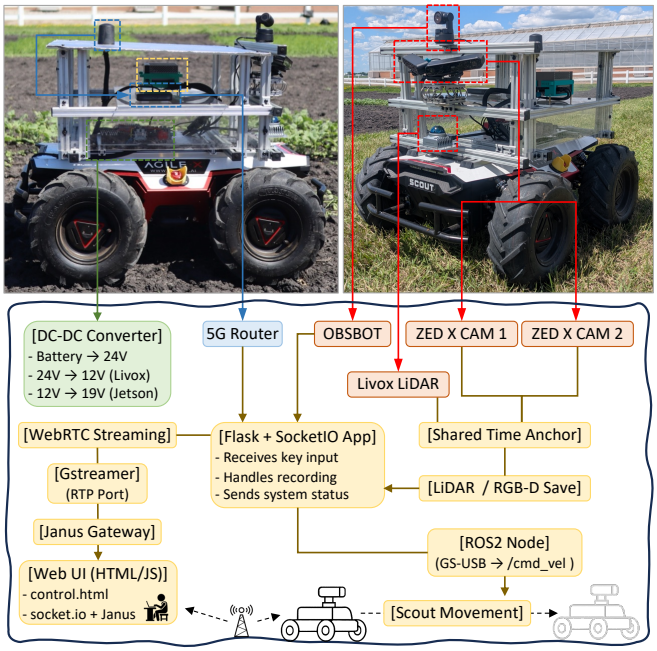

Fig. 3: System diagram of the *AgriChrono* platform showing hardware mounting locations on the robot and internal software flow for synchronized sensing, remote control, and data recording.

Air camera provides panoramic video streaming covering the forward, lateral, and downward directions. The user can remotely control the camera, enabling intuitive awareness of the robot's surroundings and facilitating efficient remote teleoperation. All control and data acquisition are performed remotely over a 5G Router with an omnidirectional antenna, maintaining stable communication during locomotion. Power is delivered via dedicated DC converters from the UGV's main battery. The system features thermal protection through a sun-shielded top panel and is enclosed in a custom aluminum-acrylic chassis, ensuring robustness for prolonged outdoor operation.

Modular Software Stack. The software stack is modular and runs on a Jetson AGX Orin 64GB embedded system. Robot control is managed via a ROS 2 Humble workspace that supports CAN-based teleoperation. A dual-camera ZED logger captures temporally synchronized `.svo2` RGB-D recordings along with per-frame IMU data, while a custom C++ module simultaneously logs LiDAR point clouds and IMU data in binary format. Sensor synchronization is achieved through a shared `sync_time.txt` file generated at session start, ensuring consistent temporal alignment across modalities. For remote operation, a WebRTC-based streaming module (Janus Gateway + GStreamer) delivers low-latency video feeds by optimizing the encoder and bitrate, while a Flask-based browser UI enables teleoperation, PTZ control, and system diagnostics. Additional system utilities include boot-time hardware initialization sequencing to prevent interface conflicts, automatic reporting of IP and network status via email, and a fail-safe mechanism that continuously monitors the network connection and immediately halts robot operation if the session is lost, ensuring safe deployment in unattended field scenarios.

B. Data Collection Protocol

Data Collection Schedule. Data were collected over a one-month period in two distinct phases. During Phase 1 (July 2–21), when crop growth was active, sampling was performed four times per day, seven days a week. In Phase 2 (July 22–August 1), as growth slowed toward maturity, sampling frequency was reduced to twice per week. Additionally, two auxiliary sites were sampled throughout the study period, with data collected once or twice per week on selected days.

Field Conditions. Data collection was suspended only during rainfall. On other days, wooden planks were placed along the traversal path to ensure robot mobility even on wet soil. To capture varying illumination, sampling was conducted

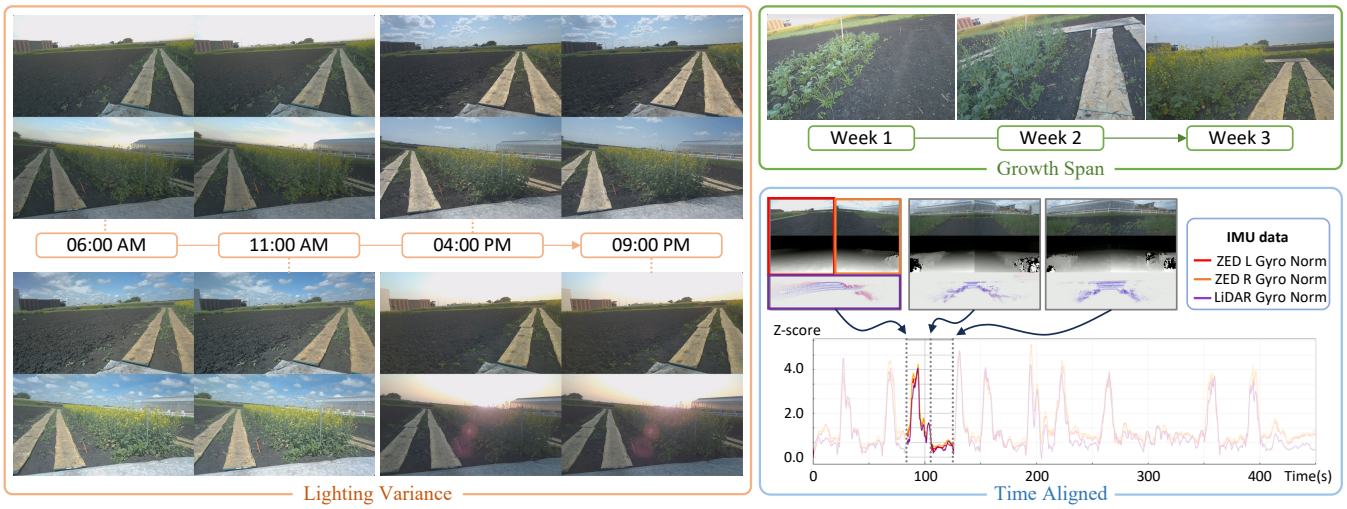

Fig. 4: Visualization of dataset properties. (i) **Lighting Variance**: RGB frames of the same scene at four times of day, showing illumination changes under natural light. The top two from the left stereo camera, the bottom two from the right stereo camera. (ii) **Growth Span**: Weekly progression (Week 1–3) of the same crop row, highlighting canopy growth and structural change. (iii) **Time Aligned**: Gyroscope magnitude (L2 norm) from IMU data of two ZED cameras and the LiDAR, Z-score normalized to verify cross-sensor alignment.

four times daily, specifically at 6:00 AM (sunrise), 11:00 AM (high sun), 4:00 PM (low sun), and 9:00 PM (sunset).

Field Site Configurations. The dataset was collected from three distinct field sites, each contributing complementary sources of variability. Site 1 served as the primary data collection site, composed of a single canola variety (*InVigor L340PC*), and one block with four rows spanning 50 ft × 3 ft. This site enabled consistent tracking of temporal appearance changes under varying growth stages and lighting conditions. Site 2 consisted of 11 blocks, each configured as a 44 ft × 3 ft plot and assigned a unique canola genotype. This layout was designed to capture morphological and structural variation across genotypes. Site 3 focused on a different crop, flax (*Gold ND*), and was organized as a 4×4 grid of plots (8 ft × 3 ft each), totaling 16 plots. In contrast to the previous sites, this configuration introduced additional structural diversity through both the crop type and its spatial arrangement.

Together, these three sites offer complementary variation across temporal, morphological, and spatial dimensions, forming a robust foundation for training models capable of generalizing across diverse field scenarios.

IV. Dataset Analysis

A. Dataset Properties

The dataset consists of time-synchronized multi-modal samples, each comprising RGB images, depth maps, LiDAR scans, and IMU readings. The RGB modality contains four images at a resolution of 1920×1080, jointly covering a horizontal field of view of $150°$. Two depth maps are included in each sample, aligned to the left cameras and computed at the same resolution using the neural depth estimation mode provided by the ZED SDK. LiDAR point clouds are available in both a forward-facing $150°$ subset and the full $360°$ scan. Owing to the non-repetitive scanning pattern of the hardware, each LiDAR measurement represents a 1 s accumulation

Site	# Sessions	FPS	Duration (s)	# Samples	Size
Site 1_{CW}	80	14.7	18,834	276,656	6.8 TB
Site 1_{CCW}	80	14.7	19,098	282,919	6.9 TB
Site 2	7	13.1	10,235	129,088	3.2 TB
Site 3	8	14.6	2,879	42,097	1.1 TB
Total	**175**	**14.3**	**51,046**	**730,760**	**18 TB**

TABLE II: Statistics of the *AgriChrono* dataset collected at the three field sites, detailing the number of recording sessions, total duration, average frame rate, total number of time-synchronized multi-modal samples (each comprising four RGB images, two depth maps, and one LiDAR scan), and overall data volume for each site.

to ensure uniform spatial coverage. IMU measurements are provided for all sensing units. Each stereo camera system records three-axis accelerometer and three-axis gyroscope data, while the LiDAR unit records three-axis gyroscope and single-axis accelerometer data. All modalities are precisely synchronized to a standard timestamp, as verified in the Time-Aligned graph of Fig.4 through the close alignment of gyroscope measurements across all three sensors.

The remainder of Fig.4 shows data from the primary site (Site 1), illustrating temporal lighting variations and morphological changes in the same crops over time. As summarized in Table II, each crop row at Site 1 was scanned twice in both clockwise(CW) and counterclockwise(CCW) directions to capture the front and rear views of the plants, resulting in a total of 160 sessions. At the remaining sites, each row was scanned once, yielding 7 sessions and 8 sessions, respectively. As a result, the *AgriChrono* dataset contains 730,760 paired samples recorded at an average rate of 14.3 FPS over approximately 51,046 s, yielding a total of 18 TB of extracted data. When counting RGB alone, this corresponds to roughly 3 million individual images. During the collection period, the vertical tilt of the cameras was adjusted to accommodate changes in crop height, ensuring consistent coverage of the plants throughout all sessions.

	Condition	Lighting Variance (Day 19)								Growth Span (6AM)					
		06:00 AM		11:00 AM		04:00 PM		09:00 PM		Day 6		Day 13		Day 20	
	Method	PSNR↑	SSIM↑	PSNR↑	SSIM↑	PSNR↑	SSIM↑	PSNR↑	SSIM↑	PSNR↑	SSIM↑	PSNR↑	SSIM↑	PSNR↑	SSIM↑
Setting 1	3D-SSS [9]	**33.5**	0.88	**30.7**	**0.89**	**31.5**	**0.87**	**34.8**	**0.90**	**31.4**	**0.87**	**32.9**	**0.91**	**32.4**	**0.90**
	3D-HGS [10]	31.9	0.82	28.6	0.79	29.7	0.79	33.2	0.85	28.8	0.72	29.9	0.75	30.6	0.80
	3D-MCMC [11]	31.7	**1.00**	27.2	0.76	29.4	0.79	32.8	0.85	27.2	0.72	27.5	0.71	29.7	0.79
	3DGS [12]	30.7	0.80	27.1	0.74	28.6	0.76	32.1	0.83	27.7	0.68	28.7	0.71	29.3	0.77
Setting 2	3D-SSS [9]	26.5	0.63	22.0	0.45	23.6	0.53	26.7	0.65	21.5	0.34	20.3	0.27	23.7	0.51
	3D-HGS [10]	26.6	0.65	22.4	0.45	23.6	0.55	27.1	0.69	22.1	0.43	21.0	0.33	24.1	0.54
	3D-MCMC [11]	**29.1**	**0.74**	**24.2**	**0.60**	**25.5**	**0.65**	**28.4**	**0.73**	**22.5**	0.41	**21.0**	**0.34**	**26.0**	**0.63**
	3DGS [12]	26.6	0.66	22.5	0.46	23.9	0.56	27.0	0.69	21.9	**0.44**	20.9	0.33	24.2	0.56
Setting 3	3D-SSS [9]	25.5	0.57	21.7	0.40	22.7	0.48	25.7	0.61	21.5	0.32	20.0	0.26	23.0	0.48
	3D-HGS [10]	25.3	0.58	21.5	0.40	22.3	0.48	25.6	0.63	21.5	0.38	19.9	0.27	22.9	0.49
	3D-MCMC [11]	**26.9**	**0.65**	**22.6**	**0.49**	**23.6**	**0.56**	**26.8**	**0.67**	**21.7**	0.35	**20.0**	**0.28**	**24.0**	**0.54**
	3DGS [12]	25.4	0.60	21.5	0.41	22.5	0.50	25.6	0.64	21.3	**0.39**	19.8	0.27	23.1	0.50
Setting 4	3D-SSS [9]	24.7	0.55	**21.3**	0.38	**21.9**	0.45	24.9	0.59	**21.5**	0.33	**19.1**	**0.26**	22.3	0.47
	3D-HGS [10]	24.1	0.54	20.8	0.37	21.2	0.44	24.4	0.59	21.0	0.32	18.9	0.25	21.9	0.46
	3D-MCMC [11]	**24.8**	**0.58**	21.2	**0.40**	21.8	**0.48**	**24.9**	**0.61**	21.0	0.31	18.8	0.25	**22.3**	**0.48**
	3DGS [12]	24.0	0.54	20.5	0.36	21.1	0.44	24.3	0.59	20.6	**0.34**	18.6	0.24	21.7	0.46

TABLE III: Novel view synthesis benchmark on *AgriChrono* (Site 1) for **Lighting Variance** and **Growth Span**. Four Gaussian Splatting methods were evaluated using PSNR and SSIM with VGGT poses. (i) **Setting 1**: trained and rendered on 15 FPS, (ii) **Setting 2**: trained on 10 FPS and rendered on 5 FPS, (iii) **Setting 3**: trained on 5 FPS and rendered on 10 FPS, (iv) **Setting 4**: trained on 3 FPS and rendered on 12 FPS. Even for training views (Setting 1), PSNR stayed in the low 30s, underscoring real-field difficulty. Results varied with lighting and growth stages, highlighting environmental sensitivity and the benchmark's value for robustness testing in dynamic outdoor scenes.

B. Dataset Structure

```
[timestamp]/
├── depth_npz_L/          ← Depth (.npz) aligned to L_L camera
│   ├── 00000.npz
├── depth_npz_R/          ← Depth (.npz) aligned to R_L camera
│   ├── 00000.npz
├── depth_png_L/          ← Depth visualization (.png), aligned to L_L
│   ├── 00000.png
├── depth_png_R/          ← Depth visualization (.png), aligned to R_L
│   ├── 00000.png
├── frame_L/              ← PNG RGB frames from left ZED X
│   ├── L_00000.png       ← L_L: left sensor of left ZED X
│   ├── R_00000.png       ← L_R: right sensor of left ZED X
├── frame_R/              ← PNG RGB frames from right ZED X
│   ├── L_00000.png       ← R_L: right sensor of left ZED X
│   ├── R_00000.png       ← R_R: right sensor of left ZED X
├── lidar/
│   ├── fov150            ← LiDAR point clouds cropped to match ZED X FoV (150°)
│   │   ├── 00000.ply     ← LiDAR point cloud for frame 0
│   ├── fov360            ← Full-range LiDAR point clouds (raw 360° FoV)
│   │   ├── 00000.ply
│   ├── lidar_info.csv    ← Per-frame timestamp and IMU data from LiDAR
├── zed_info.csv          ← Per-frame timestamp and IMU data from ZED L and R
```

Fig. 5: Public release format of the *AgriChrono dataset*

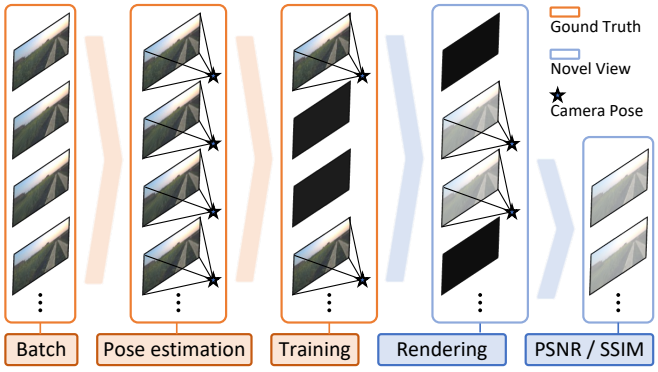

Fig. 6: Benchmarking protocol for *AgriChrono*. A 60-second (900-frame) segment is divided into ten directories (90 frames each), used for pose estimation, model training under varying FPS, novel-view rendering at unseen poses, and evaluation against ground truth.

Each session is provided as a compressed archive named `[timestamp].tar.gz`. When extracted, the dataset is organized as illustrated in Fig. 5. Depth data are stored in both `.npz` and `.png` formats, while RGB data are stored as `.png` images captured from the left and right sensors of each stereo camera. LiDAR point clouds are saved in `.ply` format within two separate directories corresponding to the different fields of view. Two accompanying `.csv` files provide the IMU measurements and timestamps for each synchronized sample within the session.

V. Benchmark

We present a new benchmark for evaluating state-of-the-art Gaussian Splatting-based methods in highly dynamic and complex real-world agricultural environments using the *AgriChrono* dataset. The dataset consists of 60-second monocular RGB sequences captured at Site 1, totaling 900 frames at 15 FPS, with all frames resized to a resolution of 512×288. The subsequent procedure follows the pipeline illustrated in Fig. 6, where each sequence was divided into 10 batches and training sets were constructed according to the target frame rate with 90 images at 15 FPS, 60 at 10 FPS, 30 at 5 FPS, and 18 at 3 FPS. The results at 15 FPS correspond to training views, while all other frame rates (10 FPS, 5 FPS, 3 FPS) are evaluated exclusively on novel views. All experiments used the same camera poses, obtained using the VGGT model, which was chosen over SfM-based methods such as COLMAP because dense clusters of dynamic objects in the scenes make feature matching unreliable.

The benchmark evaluates two core challenges in *AgriChrono*, as shown in Table III. The first is Lighting Variance, using same-day captures at four times (06:00 AM,

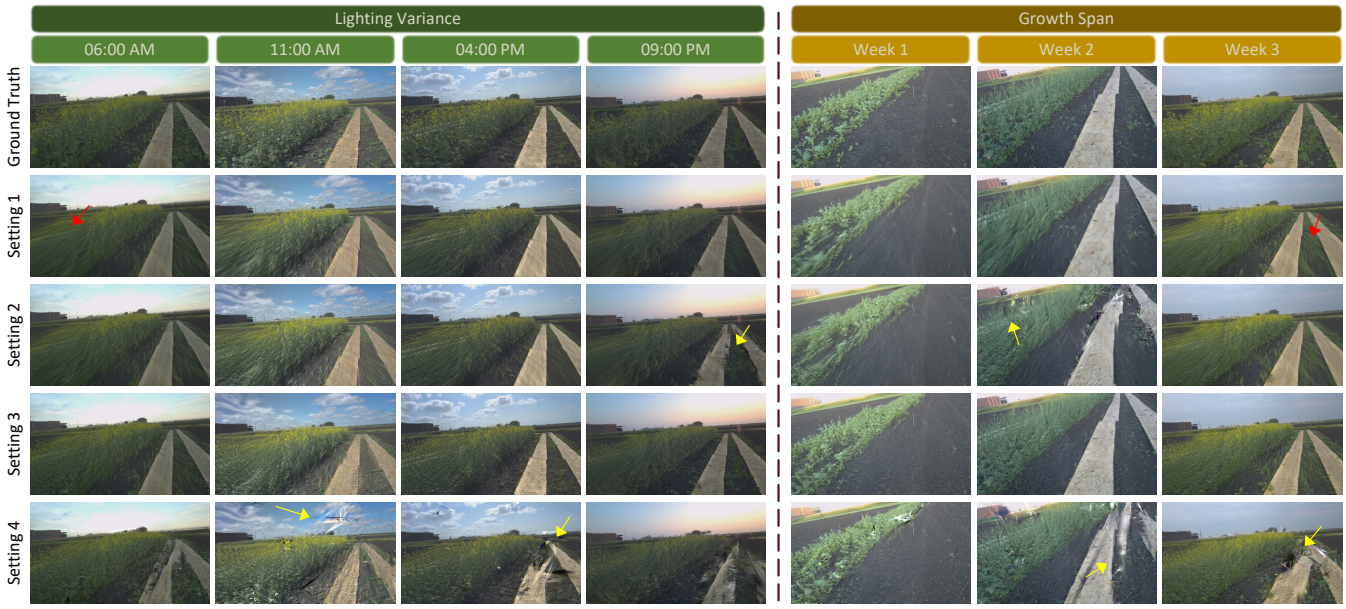

Fig. 7: Qualitative results of **3D-MCMC** [11], which generally achieved higher scores for novel-view evaluation than other methods in Table III (Settings 2–4). While the rendered images appear broadly similar to the ground truth, closer inspection reveals blurred crop structures, highlighted by **red arrows**, a symptom also visible in the training-view results (Setting 1). In novel views, the issue becomes more pronounced, showing not only blurring but also clear structural breakages, highlighted by **yellow arrows**.

11:00 AM, 04:00 PM, 09:00 PM) to assess robustness to illumination changes. The second is Growth Span, using captures at 06:00 across three growth stages one week apart (Day 6, Day 13, Day 20) to evaluate robustness under temporal morphological change. Four Gaussian Splatting methods [9], [10], [11], [12] were assessed using PSNR and SSIM between rendered and ground-truth images. Even training views achieved PSNR only in the low 30s (values above 40 are typically expected), and novel-view results were markedly lower. Performance also fluctuated with lighting and growth stage, indicating that current 3D reconstruction models face major challenges generalizing to complex agricultural scenes, with qualitative results as shown in Fig. 7. These findings highlight the novelty and practical value of *AgriChrono* as a benchmark for developing and rigorously testing models that remain robust under large illumination shifts and continuous crop growth, and we anticipate it will serve as a strong reference for future research bridging the gap between controlled performance and field deployment.

VI. Conclusions

A. Discussion

Current 3D reconstruction models in dynamic agricultural scenes with multiple moving objects struggle to maintain stable quality, with performance varying under different illumination and crop growth stages. These issues stem from existing datasets, which are primarily object-level and limited in lighting or growth conditions, and from the lack of platforms enabling stable, long-term, multi-condition, multi-sensor data collection in real farmland environments. To address this, we developed a platform that enables reliable long-term multi-modal acquisition across varied lighting and growth conditions, and we publicly released the resulting dataset. This resource provides a foundation for future work toward robust and generalizable models in complex, real-world agricultural environments.

B. Limitations

The LiDAR sensor used in this study operates in a non-repetitive scanning mode, which requires temporal accumulation. However, even after integrating over 1s intervals, the resulting point clouds remain sparse. In addition, although the dedicated SDK API was employed for IMU extraction, a firmware defect caused accelerometer readings to be available only along a single axis. Finally, despite the use of long-range remote teleoperation, data collection was still manually controlled, making it difficult to guarantee identical trajectories and viewpoints across sessions.

C. Future Works

To address current limitations, we plan to upgrade the sensing suite with a higher-performance LiDAR sensor to enable denser depth capture and calibrated, RGB-aligned ground-truth depth. We will also integrate a GPS module fused with IMU data to provide accurate ground-truth camera extrinsics. In parallel, we aim to transition from remote teleoperation to fully autonomous navigation, leveraging the ZED X stereo cameras as onboard perception sensors while reserving the streaming camera for safety monitoring. These upgrades will support more consistent, higher-quality data collection and further enhance the dataset's value for 3D reconstruction, localization, and benchmarking in dynamic agricultural environments.

REFERENCES

[1] A. Botta, P. Cavallone, L. Baglieri, G. Colucci, L. Tagliavini, and G. Quaglia, "A review of robots, perception, and tasks in precision agriculture," applied mechanics, vol. 3, no. 3, pp. 830–854, 2022.

[2] Y. Lu and S. Young, "A survey of public datasets for computer vision tasks in precision agriculture," Computers and Electronics in Agriculture, vol. 178, p. 105760, 2020.

[3] N. Heider, L. Gunreben, S. Zürner, and M. Schieck, "A survey of datasets for computer vision in agriculture," arXiv preprint arXiv:2502.16950, 2025.

[4] S. K. Panda, Y. Lee, and M. K. Jawed, "Agronav: Autonomous navigation framework for agricultural robots and vehicles using semantic segmentation and semantic line detection," in Proceedings of the IEEE/CVF Conference on Computer Vision and Pattern Recognition, 2023, pp. 6272–6281.

[5] G. Chang, T.-A. Vu, V. Alumootil, H. Song, D. Pham, S. Kim, and M. K. Jawed, "Reconstruction using the invisible: Intuition from nir and metadata for enhanced 3d gaussian splatting," arXiv preprint aeXiv:2508.14443, 2025.

[6] E. Marks, J. Bömer, F. Magistri, A. Sag, J. Behley, and C. Stachniss, "Bonnbeetclouds3d: A dataset towards point cloud-based organ-level phenotyping of sugar beet plants under real field conditions," in 2024 IEEE/RSJ International Conference on Intelligent Robots and Systems (IROS). IEEE, 2024, pp. 1804–1811.

[7] J. Zhu, R. Zhai, H. Ren, K. Xie, A. Du, X. He, C. Cui, Y. Wang, J. Ye, J. Wang et al., "Crops3d: a diverse 3d crop dataset for realistic perception and segmentation toward agricultural applications," Scientific Data, vol. 11, no. 1, p. 1438, 2024.

[8] A. Zarei, B. Li, J. C. Schnable, E. Lyons, D. Pauli, K. Barnard, and B. Benes, "Plantsegnet: 3d point cloud instance segmentation of nearby plant organs with identical semantics," Computers and Electronics in Agriculture, vol. 221, p. 108922, 2024.

[9] J. Zhu, J. Yue, F. He, and H. Wang, "3d student splatting and scooping," in Proceedings of the Computer Vision and Pattern Recognition Conference (CVPR), June 2025, pp. 21 045–21 054.

[10] H. Li, J. Liu, M. Sznaier, and O. Camps, "3d-hgs: 3d half-gaussian splatting," arXiv preprint arXiv:2406.02720, 2024.

[11] S. Kheradmand, D. Rebain, G. Sharma, W. Sun, Y.-C. Tseng, H. Isack, A. Kar, A. Tagliasacchi, and K. M. Yi, "3d gaussian splatting as markov chain monte carlo," Advances in Neural Information Processing Systems, vol. 37, pp. 80 965–80 986, 2024.

[12] B. Kerbl, G. Kopanas, T. Leimkühler, and G. Drettakis, "3d gaussian splatting for real-time radiance field rendering." ACM Trans. Graph., vol. 42, no. 4, pp. 139–1, 2023.